Chinese Journal of Aeronautics, 2013,26(3): 529–534

Chinese Society of Aeronautics and Astronautics
& Beihang University

Chinese Journal of Aeronautics

cja@buaa.edu.cn
www.sciencedirect.com

Improvement of Baldwin–Lomax turbulence model for supersonic complex flows

Zhao Rui [a], **Yan Chao** [a,*], **Yu Jian** [a], **Li Xinliang** [b]

[a] *School of Aeronautic Science and Engineering, Beihang University, Beijing 100191, China*
[b] *Key Laboratory of High Temperature Gas Dynamics, Chinese Academy of Sciences, Beijing 100190, China*

Received 9 January 2012; revised 25 April 2012; accepted 29 May 2012
Available online 30 April 2013

KEYWORDS

Baldwin–Lomax model;
Boundary layers;
Computational aerodynamics;
Entropy;
Supersonic flows;
Turbulence models

Abstract Entropy represents the dissipation rate of energy. Through direct numerical simulation (DNS) of supersonic compression ramp flow, we find the value of entropy is monotonously decreasing along the wall-normal direction no matter in the attached or the separated region. Based on this feature, a new version of Baldwin–Lomax turbulence model (BL-entropy) is proposed in this paper. The supersonic compression ramp and cavity-ramp flows in which the original Baldwin–Lomax model fails to get convergent solutions are chosen to evaluate the performance of this model. Results from one-equation Spalart–Allmaras model (SA) and two-equation Wilcox k–ω model are also included to compare with available experimental and DNS data. It is shown that BL-entropy could conquer the essential deficiency of the original version by providing a more physically meaningful length scale in the complex flows. Moreover, this method is simple, computationally efficient and general, making it applicable to other models related with the supersonic boundary layer.

1. Introduction

Advances in computer power have given rise to utilize more accurate methods of simulating and modeling turbulent flows. However, grid resolution requirements and time cost typically restrict direct numerical simulation (DNS) and even large eddy simulations (LES) to only low Reynolds numbers. That is, Reynolds Average Navier–Stokes (RANS) equations along with a turbulence model seem to be still the most powerful tool for engineering aerodynamic analysis nowadays. Among the numerous RANS models, the Baldwin–Lomax (BL) model becomes a popular algebraic eddy viscosity model for its ease of implementation, robustness, and relative accuracy. Since it was proposed in 1978,[1] BL model has been widely employed in the engineering area, whereas it fails in the following aspects[2]: (A) strong adverse pressure boundary layer flow; (B) viscous vortical flow; (C) flows in and above separated bubbles; (D) shock waves and shock waves/boundary layer interaction areas.

Many investigations have been conducted to improve the capability of the original BL model. Degani and Schiff[3] proposed the Degani–Schiff correction for turbulent vortical flows; Panaras and Steger[4] pointed out the physical deficiencies of the above correction, and proposed "Kcut correction", but it is complicated to define the "Kcut point"; later on, Panaras[5] derived a new correction for the simulation of swept shock

* Corresponding author. Tel.: +86 10 82338071.
E-mail addresses: zhaorui@ase.buaa.edu.cn (R. Zhao), yanchao@buaa.edu.cn (C. Yan), yujian@ase.buaa.edu.cn (J. Yu), lixl@lnm.imech.ac.cn (X. Li).

Peer review under responsibility of Editorial Committee of CJA.

Production and hosting by Elsevier

1000-9361 © 2013 Production and hosting by Elsevier Ltd. on behalf of CSAA & BUAA.
http://dx.doi.org/10.1016/j.cja.2013.04.047

wave/turbulent boundary layer interactions by including a reference point in the upstream of the separation region. Similarly, Shang and Hankey[6] incorporated the relaxation technique in an attempt to account for upstream turbulence history effects. Recently, You and Liang[7] proposed the shape factor to detect the separation and reattachment point, with the purpose of improving the performance of BL model in separation regions. Wong et al.[8] made a curvature correction to BL model and employed it in simulating the three-dimensional shock control bumps with reasonable results. Camelli and Löhner[9] introduced a BL–Smagorinsky model, which could be considered as a new version of RANS/LES hybrid method for unsteady flows. This idea was further developed by Li and Wu,[10] but they used the turbulence length scales as the interface function of the two models. However, most corrections above are either complex or need much experience, which may not be suitable for engineering applications.

This research focuses on the deficiencies of the BL model for supersonic complex flow, and tries to develop a simple modification to improve the overall flowfield predication. We choose supersonic compression ramp and cavity-ramp flows which are representative in the engineering area to evaluate the performance of this new model. The one-equation Spalart–Allmaras (SA) model[11] and two-equation Wilcox k–ω model[12] are also included to compare with the experimental and DNS data.

2. Numerical method

2.1. Governing equation

The three-dimensional RANS equations are solved by the finite volume method with structured grids and advanced in time by LU-SGS method. The second-order MUSCL algorithm using minmod limiter[13] and the Roe scheme[14] is used for the discretization of the inviscid terms, while the viscous terms are centrally differenced.

2.2. Baldwin–Lomax turbulence model

In the Baldwin–Lomax formation, the eddy viscosity coefficient μ_t is given by:

$$\mu_t = \begin{cases} (\mu_t)_{\text{inner}} & Y \leqslant Y_c \\ (\mu_t)_{\text{outer}} & Y > Y_c \end{cases} \tag{1}$$

where Y represents the local distance measured normal to the body surface and Y_c is the smallest value of Y where the values of $(\mu_t)_{\text{inner}}$ and $(\mu_t)_{\text{outer}}$ are equal.

For the inner region, the eddy viscosity is given by the Prandtl-Van Driest formulation:

$$(\mu_t)_{\text{inner}} = \rho(KYD)^2\Omega \tag{2}$$

where ρ is the density, Ω the magnitude of vorticity, and $K = 0.4$ the von Karman's constant. The Van Driest damping factor D is given by:

$$D = 1 - \exp(-Y\sqrt{\rho_w|\tau_w|}/26\mu_w) \tag{3}$$

where τ_w is the wall shear stress, ρ_w the density at the wall, μ_w the dynamic viscosity at the wall. In the outer region, the eddy viscosity is formulated by the following relation:

$$(\mu_t)_{\text{outer}} = \rho k C_{cp} F_{\text{wake}} F_{\text{kleb}} \tag{4}$$

The outer function F_{wake} is:

$$F_{\text{wake}} = \min(Y_{\max}F_{\max}, C_{wk}Y_{\max}U_{\text{dif}}^2/F_{\max}) \tag{5}$$

where $F_{\max} = \max(Y\Omega D)$, $Y_{\max}$ is the value of Y where $F_{\max}$ occurs, U_{dif} the difference between the maximum and minimum velocities in the profile and the Klebanoff intermittency factor F_{kleb} is given by:

$$F_{\text{kleb}} = [1 + 5.5(C_{\text{kleb}}Y/Y_{\max})^6]^{-1} \tag{6}$$

The other closure coefficients used are $k = 0.0168$, $C_{cp} = 1.6$, $C_{wk} = 1.0$, and $C_{\text{kleb}} = 0.3$.

The strength and weakness of the original BL model are well-known in the computational fluid dynamics (CFD) community: it gives reasonable accuracy for steady flows with little or no separation and performs poorly if there is a large separation. This failure may lie in two aspects. The constants appearing in the model are deduced for constant pressure boundary layers at transonic speeds and may not be suitable for supersonic or hypersonic complex flows. And, the outer eddy viscosity $(\mu_t)_{\text{outer}}$ depends directly on the value of $F_{\max}$ and $Y_{\max}$. In the original BL model, there is no limit while searching the proper $F_{\max}$, which may confuse length scale $Y_{\max}$ in the complex flow. Fig. 1 shows the DNS result of the supersonic flow past the 24° ramp at Mach number $Ma = 2.90$,[15] where X, Y are Cartesian coordinates, $\delta = 6.5$ mm is the boundary layer thickness at the reference location $X = -30$ mm, and the subscript "∞" denotes the quantity in the freestream. The distributions of quantities are extracted at different locations ($X/\delta = -4.6$, -2.0, -1.0, 0) normal to the wall, and could be found that function F (nondimensionalized by the freestream velocity U_∞) displays several extrema on the upstream of and throughout the separation region while entropy S ($S = p/\rho^r$, p is the pressure and $r = 1.4$ is the specific heat ratio) exhibits a monotone characteristic (see Fig. 2). Since the values of these extrema may differ by one order of magnitude, the unlimited search of $F_{\max}$ and $Y_{\max}$ will result in unphysical discontinuous eddy viscosity through the streamwise direction.

The aim of the present work is to introduce an effective method to limit the search range of F, and then enlarge the capability of BL model in simulating the supersonic complex flow. S represents the dissipation rate of energy. Due to the supersonic turbulent fluctuation and skin friction near the wall, the value of S is much larger in the boundary layer than

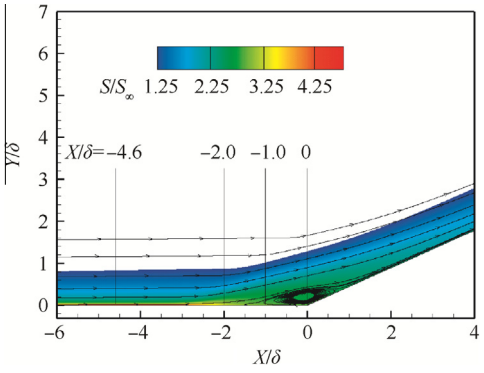

Fig. 1 Entropy contour of compression ramp (only depict $S/S_\infty > 1.0/0.8$).

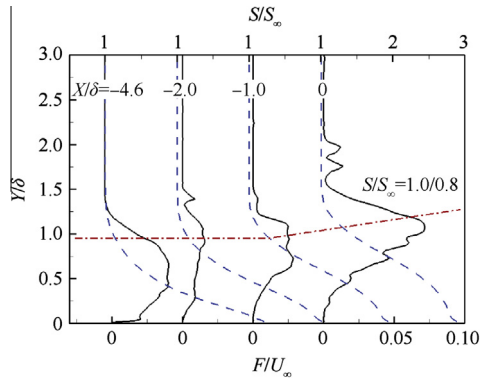

Fig. 2 Function F and entropy S distributions normal to the wall at different locations.

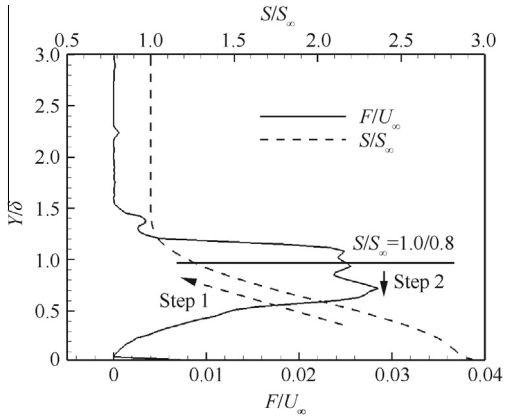

Fig. 3 Search steps used in BL-entropy ($X/\delta = -1.0$).

that in the outer flow including the regions behind the shock waves. What is more, the distribution of S displays a monotone feature normal to the wall no matter in the attached flow or the separation area. Thus, S seems to be a "perfect criterion" to limit the search range of F.

To illustrate the search method, the distributions of the above two quantities at $X/\delta = -1.0$ are shown in Fig. 3. The process is divided into two steps.

First, S goes along the wall-normal direction until $S/S_\infty = C$ (C is an empirical parameter), saving up the location (Step 1). Then, F goes back from this location and gets the F_{max} and Y_{max} (Step 2). The essential idea of this new method, termed as BL-entropy, is to take advantage of the characteristic of S to define the boundary layer. Accordingly, the value of C follows the definition of boundary layer by velocity profiles ($U/U_\infty = 0.95$, U is the streamwise velocity), while the performance of BL-entropy is not sensitive to this value with the range of 1.0/0.75–1.0/0.95. We suggest the constant $C = 1.0/0.8$ after our numerical experiments (see Figs. 2 and 4) and $C_{cp} = 2.08$ for supersonic flows advised by Ref.[5]

3. Results and discussion

3.1. Supersonic flat plate ($Ma = 2.25$)

This test case is used to validate the performance of BL-entropy in stable boundary layer flows, which should be consistent

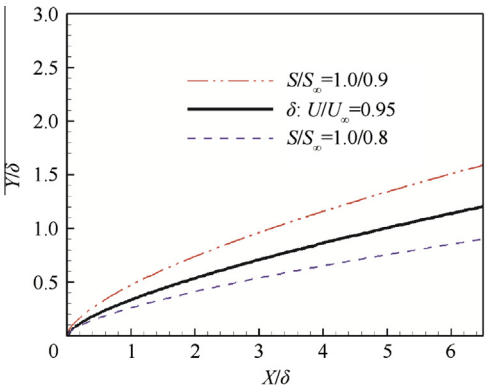

Fig. 4 Comparison of boundary layer and iso-entropy layers.

with the original one. Pirozzol et al.[16] have simulated a flat plate boundary layer with free stream $Ma = 2.25$ and Reynolds number $Re = 63500$/in. (in.: inch) through DNS approach. The same flow condition is adopted for the present computation. After van Direst transformation, i.e., $U^+_{vd} = \int_0^{u^+} (\rho/\rho_w)^{1/2} du^+$, where U^+_{vd} is the friction velocity after the van Direst transformation, $u^+ = \frac{U}{\sqrt{\tau_w/\rho}}$ is the wall friction velocity, the velocity profiles along the distance to the wall ($Y^+ = Y\sqrt{\tau_w \rho}/\mu$) at $X = 8.8$ in. are illustrated in Fig. 5.

For this simple flow, BL-entropy and the original one obtain the same velocity profiles since the length scale Y_{max} is one and only. Fig. 5 depicts the thickness of boundary layer ($\delta = U/U_\infty = 0.95$) and iso-entropy layers ($S/S_\infty = 1.0/0.8$ and $S/S_\infty = 1.0/0.9$) in the streamwise direction. The limiter $C = 1.0/0.8$ chosen here can strictly limit the search range in the boundary layer to get physical meaningful length scales.

3.2. Supersonic compression ramp flow ($Ma = 2.90$)

The interaction of shock waves and turbulent boundary layers is a classical problem of fluid mechanics, which also has practical importance in such areas as inlet design, external aerodynamics, and turbomachinery. Li et al.[15] have performed DNS method to simulate the supersonic flow past the compression ramp. The incoming flow conditions are listed in Table 1, also including the reference experiment of Bookey et al.[17] An equilibrium supersonic turbulent flow approaches a compression ramp. The deflection of the flow by the ramp generates a shock system. For sufficiently large pressure rise, the boundary layer

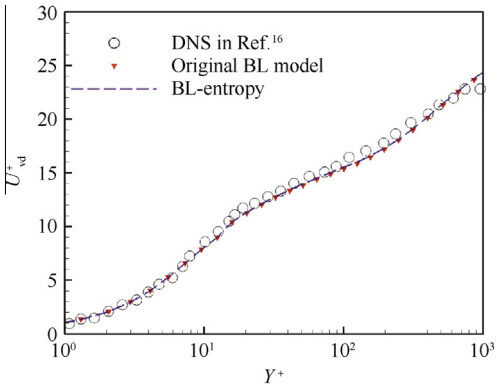

Fig. 5 Streamwise velocity profile at $X = 8.8$ in.

Table 1 Conditions for incoming turbulent boundary layer (at $X = -30$ mm).

Method	Ma_∞	Re_θ	θ (mm)	δ (mm)	T_∞ (K)	T_{wall} (K)
DNS	2.9	2344	0.42	6.5	108.1	307
Experiment	2.9	2400	0.43	6.7	108.1	307

Note: Re_θ: Reynolds number based on momentum thickness; θ: momentum thickness; T_∞: temperature in the freestream; T_{wall}: wall temperature.

separates and a λ-shock forms (see Fig. 1). The grids are clustered around the corner and ramped regions, with the first grid line to the wall Y^+ less than 1.0.

The calculation of original BL model is not converged for this supersonic complex flow. The entropy could predict a reasonable boundary layer region to limit the search range of the length scales (see Fig. 1). As a result, the eddy viscosity produced by BL-entropy is strictly limited around the wall, similar to those of SA model and Wilcox k–ω model see Fig. 6. Nevertheless, with the basic hypothesis of local balance between turbulent movement and the mean flow in the framework of algebraic turbulence model, the eddy viscosity produced by BL-entropy is fluctuating and less than those of the other two models. On the other hand, Wilcox k–ω model produces too much eddy viscosity to resist separation (see Fig. 6), also reflecting on the most "fullness" velocity distributions approaching the corner (see Fig. 7). Both BL-entropy and SA model predict consistent velocity profiles with DNS results.

Fig. 8 compares the wall pressure distributions. The midpoint of the pressure rise coincides roughly with the reattachment location, while the rise itself is indicative of the recovery rate of the boundary layer downstream of the reattachment.[18] In accordance with the previous remarks, the pressure predicted by Wilcox k–ω model recovers the most quickly, followed by the results of SA model and BL-entropy. Again, BL-entropy gives a sound pressure distribution, compared with experimental and DNS data.

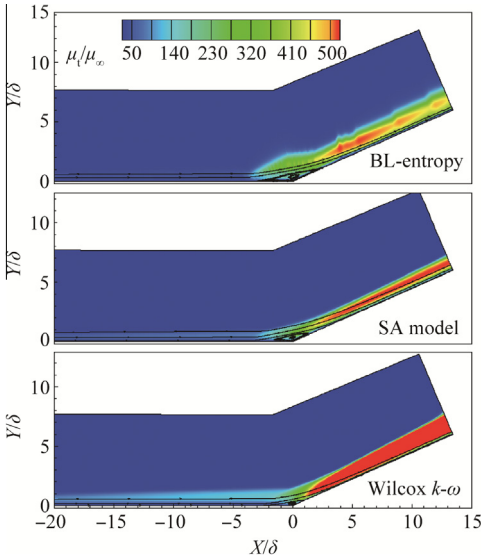

Fig. 6 Comparisons of eddy viscosity distributions and recirculation areas around the corner.

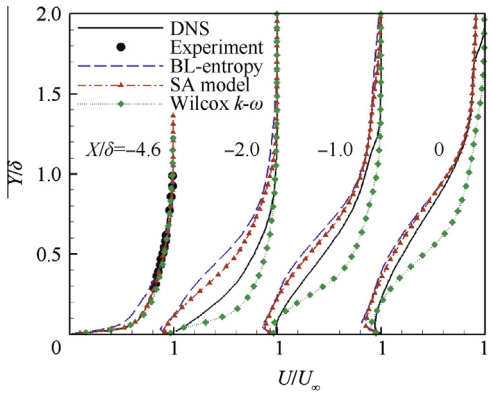

Fig. 7 Streamwise velocity profiles at different locations.

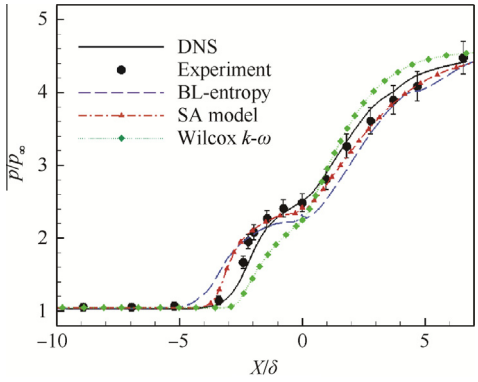

Fig. 8 Comparison of wall-pressure distributions.

3.3. Supersonic cavity-ramp flow ($Ma = 2.92$)

The cavity-ramp configurations are considered as key components for next-generation hypersonic vehicles, such as scramjets and ramjets. With such devices, recessed cavities may be used to provide flame stabilization. Settles et al.[19] have carried out the corresponding experiments and the incoming flow conditions are listed in Table 2. Fig. 9 presents the Mach number contours. The dominant feature of the flow is the free-shear layer, under which a large recirculation zone fills almost the whole cavity. In Fig. 9, X' is the inclined coordinate direction, parallel to the ramp surface. On the ramped portion of the cavity, the free-shear layer reattaches to form a turbulent boundary layer while a compression fan coalesces into a shock wave downstream of the reattachment point. The grids are clustered to the cavity and ramped regions, with Y^+ of the first grid line to the wall less than 1.0.

For this complex flow, the original BL model fails to give a convergent solution again. The entropy is concentrated in the

Table 2 Incoming flow conditions for supersonic cavity-ramp flow ($X = -25.4$ mm).

Ma_∞	Re	δ_{ref} (mm)	p_∞ (Pa)	T_∞ (K)
2.92	6.7×10^7	2.9	21240	95.37

Note: δ_{ref}: boundary layer thickness at the reference location $X = -25.4$ mm.

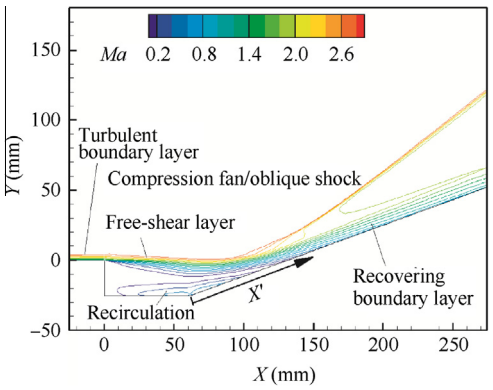

Fig. 9 Flow structures for cavity-ramp (Mach number contours).

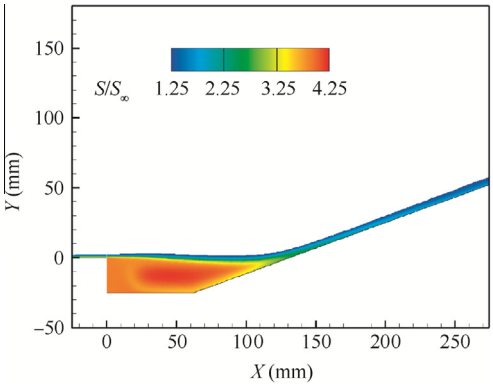

Fig. 10 Entropy contours around cavity-ramp (only depict $S/S_\infty > 1.0/0.8$).

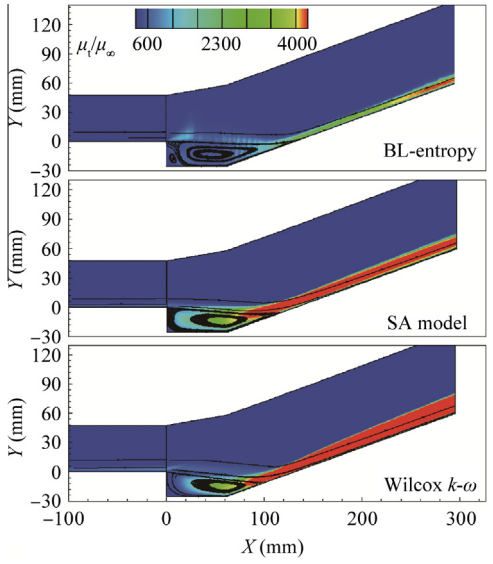

Fig. 11 Comparisons of eddy viscosity distributions and recirculation areas around the cavity-ramp.

whole cavity area due to the low-speed recirculation flow which contains much less mechanical energy (see Fig. 10). Accordingly, the boundary layer region denoted by

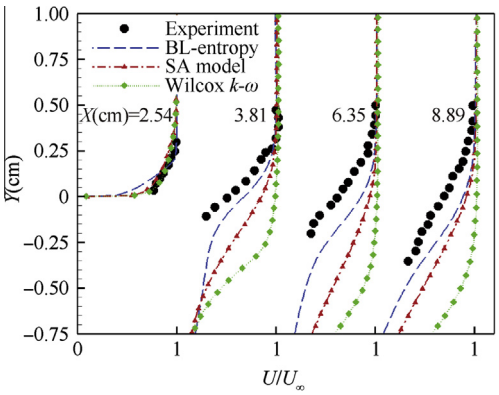

Fig. 12 Streamwise velocity profiles at different locations.

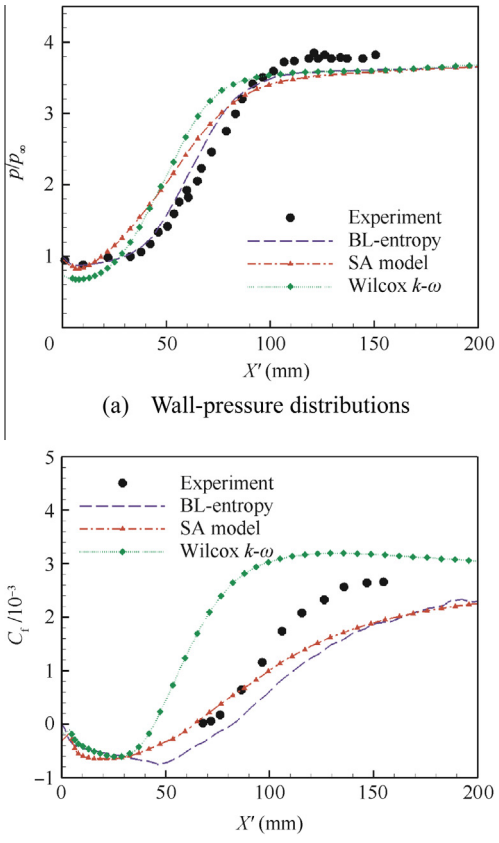

Fig. 13 Comparison of wall-pressure and skin-frication coefficients along the wall.

$S/S_\infty > 1.0/0.8$ is too large to limit the length scale in this area, leading to an absence of modeled eddy viscosity compared with those of SA model and Wilcox k–ω model (see Fig. 11). However, this limiter $C = 1.0/0.8$ is strict enough to get rid of the entropy increment where the flow passes the oblique shock waves, predicting a reasonable recovered boundary layer along the ramped portion (see Fig. 10). Among the three models, Wilcox k–ω produces the most eddy viscosity along the ramped region while excessive viscosity is predicted in the cavity area by SA model.

Fig. 12 presents streamwise velocity profiles within the shear layer prior to reattachment. Here, all of the three models underestimate the initial growth of the shear layer and the degree of its displacement into the outer core flow, whereas BL-entropy provides generally better predictions than those of SA and Wilcox k–ω model.

Fig. 13(a) shows the comparisons of wall pressure on the ramped portion. The calculated pressure distributions by Wilcox k–ω and SA models recover dramatically due to the overabundant eddy viscosity produced along this portion, while BL-entropy provides quite good predication. Comparing the skin-frication coefficient distributions (see Fig. 13(b)), we could find Wilcox k–ω model results in the smallest recirculation zone (also denoted in Fig. 11), while the performances of BL-entropy and SA model are satisfied to predict the separation but inferior after reattachment. In Fig. 13, C_f is the skin frication coefficient.

4. Conclusions

(1) Entropy is the index of energy dissipation. Through direct numerical simulation of the supersonic ramp flow, the value of entropy is much larger at the wall than that in the outer flow, while it keeps numerical monotone in the wall normal direction. This character could be introduced to denote the supersonic boundary layer.
(2) Within the framework of the algebraic eddy viscosity concept, we utilize this entropy concept to limit the length scales of BL model into the interior of boundary layer and propose BL-entropy. This simple modification improves the overall flowfield prediction, validated by simulating the test cases in which the original one is incapable.
(3) This new correction is simple, computationally efficient and general, making it applicable to other models related with the supersonic boundary layer.
(4) The behavior of entropy in the low-speed and hypersonic complex flows should be further investigated, especially the unfavorable effect of entropy increment caused by strong shock waves. These will be left for our future work, with the aim to extend the capability of this method.

Acknowledgements

This study was co-supported by National Basic Research Program of China (No. 2009CB724104), the Innovation Foundation of BUAA for Ph.D. Graduates (No. 300521), and the Academic New Artist Award of BUAA for Ph.D. Graduates.

References

1. Baldwin BS, Lomax H. Thin layer approximation and algebraic model for separated turbulent flows. AIAA-1978-257; 1978.
2. Wilcox DC. *Turbulence modeling for CFD*. 3rd ed. California: DCW Industries, Inc.; 2006.
3. Degani D, Schiff LB. Computation of supersonic viscous flows around pointed bodies at large incidence. AIAA-1983-34; 1983.
4. Panaras AG, Steger JL. A thin-layer solution of the flow about a prolate spheroid. *Z Flugwiss* 1988;**12**:173–80.
5. Panaras AG. Algebraic turbulence modeling for swept shock-wave/turbulent boundary-layer interactions. *AIAA J* 1997;**35**(2):456–63.
6. Shang Jr J, Hankey WL. Numerical solution for supersonic turbulent flow over a compression ramp. *AIAA J* 1975;**10**(13):1368–74.
7. You YC, Liang DW. The application of improved BL algebraic turbulence model in three-dimensional separated flows. In: *The key technology of large aircraft, and China Aviation Society forum annual meeting 2007 proceedings;* 2007 [Chinese].
8. Wong WS, Qin N, Sellars N, Holden H, Babinsky H. A combined experimental and numerical study of flow structures over three-dimensional shock control bumps. *Aerosp Sci Technol* 2008;**12**:436–47.
9. Camelli FE, Löhner R. Combining the Baldwin–Lomax and Smagorinsky turbulence models to calculate flows with separation regions. AIAA-2002-426; 2002.
10. Li B, Wu SP. Hybrid RANS/LES model based on turbulent scale. *J Beijing Univ Aeronaut Astronaut* 2008;**34**(7):755–8 [Chinese].
11. Spalart PR, Allmaras SR. A one-equation turbulence model for aerodynamic flows. AIAA-1992-439; 1992.
12. Wilcox DC. Reassessment of the scale determining equation for advanced turbulence models. *AIAA J* 1988;**26**(11):1299–310.
13. Jameson A. Artificial diffusion, upwind biasing, limiters and their effect on accuracy and multigrid convergence in transonic and hypersonic flows. AIAA-1993-3359; 1993.
14. Roe PL. Approximate Riemann solvers, parameter vectors and difference schemes. *J Comput Phys* 1981;**43**(2):357–72.
15. Li XL, Fu DX, Ma YW, Liang X. Direct numerical simulation of shock-boundary layer interaction around the supersonic ramp. *Sci China* 2010;**40**(6):791–9 [Chinese].
16. Pirozzoli S, Grasso F, Gatski TB. Direct numerical simulation and analysis of a spatially evolving supersonic turbulent boundary layer at $M = 2.25$. *Phys Fluids* 2004;**16**(3):530–45.
17. Bookey PB, Wychham C, Smits AJ. New experimental data of STBL at DNS/LES accessible Reynolds numbers. AIAA-2005-309; 2005.
18. Fan TC, Tian M, Edwards JR, Hassan HA, Baurle RA. Validation of a hybrid Reynolds-average/large-eddy simulation method for simulating cavity flameholder configurations. AIAA-2001-2929; 2001.
19. Settles GS, Williams DR, Baca BK, Bogdonoff SM. Reattachment of a compressible turbulent free shear layer. *AIAA J* 1982;**20**(1):60–7.

Zhao Rui is a Ph.D. student at School of Aeronautic Science and Engineering, Beihang University. He received his B.S. degree from the same university in 2008. His current research interests include turbulence modeling and RANS/LES hybrid method.

Yan Chao is a professor and Ph.D. supervisor at School of Aeronautic Science and Engineering, Beihang University. He received his Ph.D. degree from Tsinghua University in 1989. Then he worked as a post-doctoral researcher in Poitier University of France for several years. His current research interests include high-order accuracy schemes, unsteady flow, LES, hybrid grid and optimization of aircraft.

Yu Jian is a postdoctoral researcher at School of Aeronautic Science and Engineering, Beihang University. He received his B.S. degree in 2006 and Ph.D. degree in 2011 from the same university. His current research interests include high-order schemes and aerodynamics.

Li Xinliang is a senior researcher and Ph.D. supervisor at Institute of Mechanics, Chinese Academy of Sciences. He received his Ph.D. degree from the same institute in 2000. Then he worked as a JSPS special researcher in Tokyo Institute of Technology from 2005 to 2007. His current research interests include compressible turbulent flow, transition prediction and aerodynamics.